

# First Principles Study of Zn-Sb Thermoelectrics

Seong-Gon Kim

UES, Inc. and Code 6691, Complex Systems Theory Branch, Naval Research Laboratory, Washington, D.C. 20375-5000

I.I. Mazin

CSI, George Mason University and Code 6691, Complex Systems Theory Branch, Naval Research Laboratory, Washington, D.C. 20375-5000

D.J. Singh

Code 6691, Complex Systems Theory Branch, Naval Research Laboratory, Washington, D.C. 20375-5000

(Received September 11, 1997)

We report first principles LDA calculations of the electronic structure and thermoelectric properties of  $\beta$ -Zn<sub>4</sub>Sb<sub>3</sub>. The material is found to be a low carrier density metal with a complex Fermi surface topology and non-trivial dependence of Hall concentration on band filling. The band structure is rather covalent, consistent with experimental observations of good carrier mobility. Calculations of the variation with band filling are used to extract the doping level (band filling) from the experimental Hall number. At this band filling, which actually corresponds to 0.1 electrons per 22 atom unit cell, the calculated thermopower and its temperature dependence are in good agreement with experiment. The high Seebeck coefficient in a metallic material is remarkable, and arises in part from the strong energy dependence of the Fermiology near the experimental band filling. Improved thermoelectric performance is predicted for lower doping levels which corresponds to higher Zn concentrations.

There has been a recent revival of activity in the search for improved thermoelectric materials, with an emphasis on new materials systems<sup>1</sup>. The efficiency of a thermoelectric is characterized by a dimensionless figure of merit,  $ZT = \sigma S^2 T / \kappa = S^2 / L$ , where  $T$  is the temperature,  $\sigma$  is the electrical conductivity,  $S$  is the Seebeck coefficient (thermopower) and  $\kappa$  is the thermal conductivity, which contains both electronic and lattice contributions,  $\kappa = \kappa_{\text{el}} + \kappa_{\text{lat}}$ . The ratio  $L = \kappa / \sigma T$ , which is often called the Lorentz number, is ordinarily limited from below by its electronic value,  $\kappa_{\text{el}} / \sigma T$ , given by the Wiedemann-Franz value,  $L = (\pi^2 / 3) (k_B / e)^2$ . Current thermoelectric materials have  $ZT \approx 1$ . With the Wiedemann-Franz value for  $L$ ,  $ZT > 1$  requires  $S > 160 \mu\text{V/K}$ . Since doped semiconductors naturally have large thermopower, much of the thermoelectric research over the past 40 years has focused on covalent semiconducting compounds and alloys, composed of 4th and 5th row elements, with a view to finding low thermal conductivity materials that have reasonable carrier mobilities and high band masses, e.g. Bi<sub>2</sub>Te<sub>3</sub>, Si-Ge and PbTe compounds. Despite the research efforts spanning three decades, little progress in increasing  $ZT$  has been achieved until recently, and in particular Bi<sub>2</sub>Te<sub>3</sub>/Sb<sub>2</sub>Te<sub>3</sub> has remained as the material of choice for room temperature applications.

In the last two years, however, three new materials with  $ZT \gtrsim 1$  have been reported<sup>2-4</sup>, and these do not clearly fall into the same class as previous thermoelectric materials. One of these novel materials,  $\beta$ -Zn<sub>4</sub>Sb<sub>3</sub>, with

reported  $ZT \approx 1.3$  at temperature relevant to waste heat recovery, has a large region of linear temperature dependence of the resistivity (Fig. 1), suggestive of a metallic rather than semiconducting material. But unlike normal metals this is accompanied by high thermopowers.

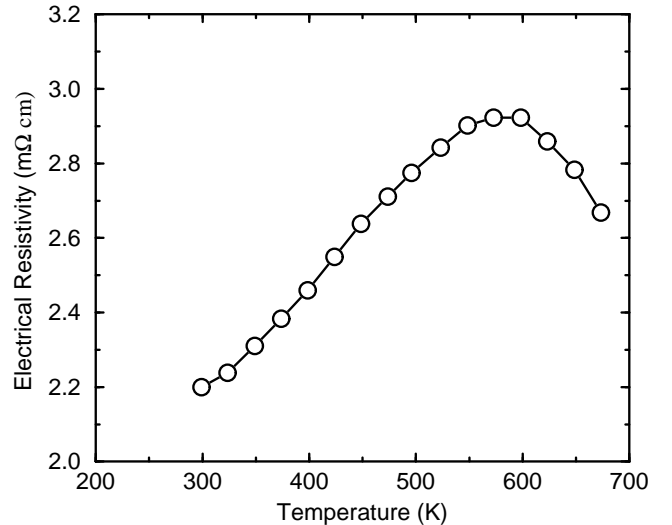


FIG. 1. Experimental resistivity of  $\beta$ -Zn<sub>4</sub>Sb<sub>3</sub>. Replotted with a linear temperature scale using data of Ref. [2].

In this report, we present first principles calculations, within the local density approximation (LDA), similar to our previous calculations for binary and filled skutterudites<sup>5-8</sup>. Our main purpose is to understand the rather remarkable thermoelectric properties of  $\beta$ -Zn<sub>4</sub>Sb<sub>3</sub> by analysing its transport properties based on electronic band structures.

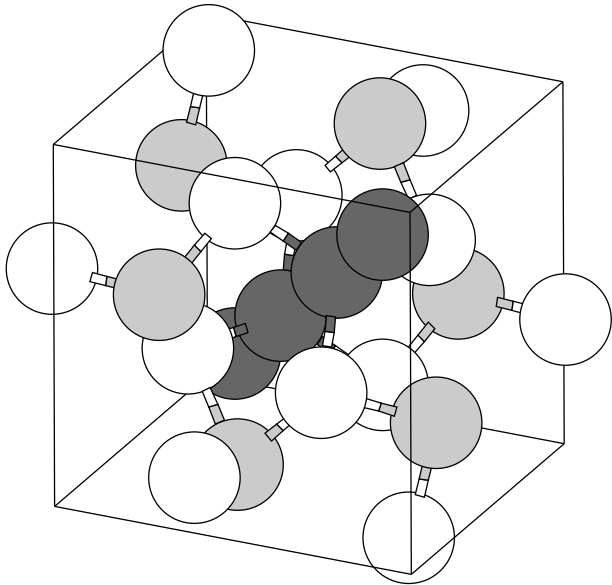


FIG. 2. Crystal structure of  $\beta$ -Zn<sub>4</sub>Sb<sub>3</sub>. White and dark grey spheres denotes the 12 Zn and 4 Sb atoms on pure sites in the 22 atom rhombohedral unit cell. 6 light grey spheres are occupied by 89% of Sb and 11% of Zn atoms.

The computations were performed self-consistently within the LDA using the general potential linearized augmented plane waves (LAPW) method<sup>9,10</sup>. This method makes no shape approximations to either the potential or charge density and uses flexible basis sets in all regions of space. As such it is well suited to materials with open crystal structures and low site symmetries like  $\beta$ -Zn<sub>4</sub>Sb<sub>3</sub>. Special care has been taken to obtain a well converged basis set of approximately 2100 functions with LAPW sphere radii of 2.5 a.u. for both Zn and Sb atoms. During the self-consistency iterations, the Brillouin-zone integrations were carried out with 10 special  $\mathbf{k}$  points in the irreducible wedge of the Brillouin zone; 781 inequivalent  $\mathbf{k}$  points were used to calculate Fermi surface averages. Use of this relatively large number of  $\mathbf{k}$  points was necessary to obtain accurate Fermi velocities, and, especially, reliable Hall coefficients. We used the local orbital extension<sup>11</sup> of LAPW method to relax linearization errors in general and to include the upper core states consistently with the valence states. The calculations were based on the experimental crystal structure of  $\beta$ -Zn<sub>4</sub>Sb<sub>3</sub><sup>13</sup> shown in Fig. 2; however, the

site reported to have approximately 11% of Zn and 89% of Sb (light grey spheres in Fig. 2) in the actual structure was taken to be a pure Sb site. This adjustment yields a formula Zn<sub>6</sub>Sb<sub>5</sub> with 22 atoms per rhombohedral unit cell. The mixed occupancy was accounted for in a rigid band model as discussed below. Of the five Sb atoms three occupy the mixed site (Sb<sup>(m)</sup>), and two reside in a pure Sb site (Sb<sup>(p)</sup>) which is crystallographically inequivalent. Two Sb<sup>(p)</sup> atoms form Sb<sub>2</sub><sup>(p)</sup> dimers parallel to the rhombohedral axis. The bond length between these two Sb atoms is 2.82 Å, which is exactly twice of Sb covalent radius. This suggest covalent Sb<sup>(p)</sup>-Sb<sup>(p)</sup> bonding, which is confirmed by the band structure calculations. Each Sb<sup>(p)</sup> forms three additional bonds with Zn, thus being essentially four-fold coordinated. The partial densities of states (Fig. 3) shows that these bonds are also largely covalent.

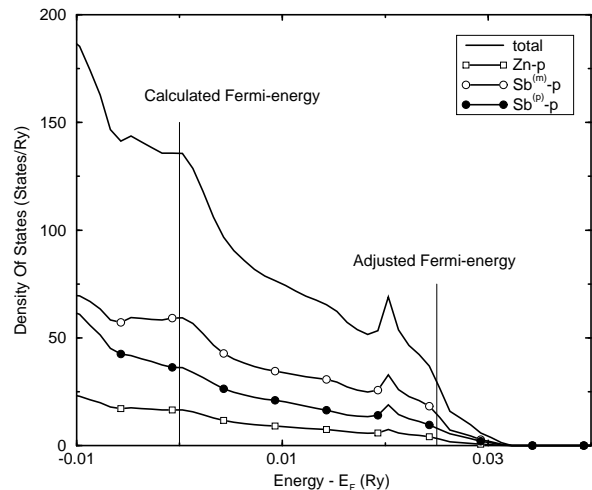


FIG. 3. Total and partial density of states of  $\beta$ -Zn<sub>4</sub>Sb<sub>3</sub>. Total density of states is for 22 atom unit cell and partial density of states are for each inequivalent atom and magnified by a factor 10 for clarity. Note the highly covalent character of the band structure. The calculations were performed for the stoichiometric composition ( $E_F$  at lower vertical line). The actual Fermi energy is given by the upper marker.

Both the Zn and Sb<sup>(m)</sup> occur in high coordinated positions; Zn forms one bond with Sb<sup>(p)</sup>, one bond with another Zn, and 3 bonds with Sb<sup>(m)</sup>, while Sb<sup>(m)</sup> forms all six bonds with Zn. The similar coordination of Zn and Sb<sup>(m)</sup> favors for Zn to substitute on Sb<sup>(m)</sup> over Sb<sup>(p)</sup>, as observed. Substituting one Sb<sup>(m)</sup> by a Zn eliminates 6 Zn-Sb bonds and creates 6 Zn-Zn bonds. In general, this is not an energetically favorable process, and one could expect stoichiometric compound Zn<sub>6</sub>Sb<sub>5</sub> rather than Zn-enhanced Zn<sub>6.33</sub>Sb<sub>4.77</sub>, as observed experimentally. On the other hand, in the stoichiometric compound, as discussed below, the bonding states of Sb are not yet com-

pletely filled, and doping electrons into the system produces an additional bonding effect. In other words, substituting Sb by Zn reduces the number of Zn-Sb bonds, but makes the remaining bonds stronger. The balance between the two effects may account for the partial substitution, however, the very narrow range of compositions for which samples exist remains unexplained in terms of the calculations.

As mentioned, our calculations were done for the stoichiometric structure. The Fermi level lies  $\approx 0.4$  eV below the top of the valence band, which is separated by a sizeable gap (also  $\approx 0.4$  eV) from the conduction bands. The effect of the deviation from stoichiometry can be taken into account in a rigid band model: it is assumed that the electronic structure of the actual compound is the same as for the stoichiometric one, the only difference being position of the Fermi level. This is expected to be valid in a highly covalent, broad band system as we find, and is supported *a posteriori* by the comparison with experiment. Correspondingly we have calculated the relevant transport properties as functions of the Fermi level position, and used the experimental Hall conductivity to find the Fermi level position corresponding to actual samples.

The relevant transport properties were determined from the calculated band structures using the standard kinetic theory as given by Ziman and others<sup>16,17</sup>. For the electrical conductivity, the Bloch-Boltzmann kinetic equation in lowest order along  $x$ -direction is (similarly for the other Cartesian directions)

---


$$\sigma_H = \frac{e^3}{12} \int d\epsilon N(\epsilon) \mathbf{v}(\epsilon) \cdot [\text{Tr}(\mathbf{M}^{-1}) - \mathbf{M}^{-1}] \cdot \mathbf{v}(\epsilon) \tau^2(\epsilon, T) \left[ -\frac{\partial f(\epsilon)}{\partial \epsilon} \right] \quad (5)$$

where for simplicity we have given the expression for cubic symmetry. Here  $\mathbf{M}$  is the  $\mathbf{k}$ -dependent effective mass tensor, defined as

$$\mathbf{M}_{\alpha\beta}^{-1} \equiv \hbar^{-1} \frac{\partial v_\alpha}{\partial k_\beta} \equiv \hbar^{-2} \frac{\partial^2 \epsilon_k}{\partial k_\alpha \partial k_\beta} \quad (6)$$

Provided that the Fermiology does not vary strongly on the scale of  $k_B T$ , the derivatives of the Fermi distribution in the above expressions may be replaced by the  $T = 0$  limit, which is the delta function, thereby suppressing the energy integrals. This approximation was used in the calculations of the Hall concentrations in this paper. However, in the expression for the Seebeck coefficient,  $S$ , one has to include the energy dependence explicitly at temperatures several times smaller than the characteristic electronic energy scale. Thus we have used the full expression,

$$\sigma_x(T) = e^2 \int d\epsilon N(\epsilon) v_x^2(\epsilon) \tau(\epsilon, T) \left[ -\frac{\partial f(\epsilon)}{\partial \epsilon} \right]. \quad (1)$$

Here  $N(\epsilon)$  is the density of electronic states at the energy  $\epsilon$  per unit volume,  $\tau$  is the scattering rate for electrons, and the quantity  $v_x^2(\epsilon)$  is defined by:

$$N(\epsilon) v_x^2(\epsilon) = \frac{2}{(2\pi)^3} \int v_x^2 \frac{dS_\epsilon}{v_\epsilon} \quad (2)$$

$$N(\epsilon) = \frac{2}{(2\pi)^3} \int \frac{dS_\epsilon}{v_\epsilon} \quad (3)$$

The integrations are carried out over the iso-energy surface,  $dS_\epsilon$ , defined by  $\epsilon_{\mathbf{k}} = \epsilon$ . For  $\epsilon_{\mathbf{k}} = E_F$ , the Fermi energy, the integral is over the Fermi surface and  $v_\epsilon$  is the Fermi velocity. In this case it is related to the square of the plasma frequency  $\omega_{p_x}^2 = 4\pi e^2 N(E_F) v_x^2(E_F)$ , which is proportional to the optical carrier concentration  $(n/m)_{\text{eff}} = N(E_F) v_x^2(E_F)$ . We note that in general this does not have a simple relationship to the Hall concentration or the electron count (i.e. the doping level); the Hall concentration is a measure of the average curvature of the Fermi surface, while the doping level is determined by the volume enclosed by the Fermi surface.

For isotropic scattering, which is often a reasonable approximation, the relaxation time does not enter the expression for the Hall concentration, yielding<sup>18,17</sup>:

$$n_H = -\sigma^2 / e\sigma_H \quad (4)$$

with

---


$$S(T) = \frac{1}{eT\sigma(T)} \int d\epsilon \epsilon \sigma(\epsilon, T) \left[ -\frac{\partial f(\epsilon)}{\partial \epsilon} \right] \quad (7)$$

where

$$\sigma(\epsilon, T) = e^2 N(\epsilon) v_x^2(\epsilon) \tau(\epsilon, T) \quad (8)$$

is the conductivity corresponding to a Fermi level positioned at  $\epsilon$ . The expression for  $\sigma(\epsilon, T)$  in Eq. (8) contains two energy dependent factors; a factor related to the square of plasma frequency,  $\omega_{p_x}^2 = 4\pi e^2 N v_x^2$  and the relaxation time,  $\tau$ . Ordinarily, the first term is the most energy dependent, but there are exceptions<sup>19</sup>, e.g. Pd metal where  $E_F$  occurs near a very sharp feature in  $N(\epsilon)$  and Kondo systems where there is resonant scattering<sup>17</sup>. Since  $\beta\text{-Zn}_4\text{Sb}_3$  does not show any indication of such behavior, we have approximated the energy dependence of  $\sigma$  using only the  $N v_x^2$  term.

$\beta\text{-Zn}_4\text{Sb}_3$  has a small Hall number and is characterized either as a low carrier density metal or a heavily doped semiconductor. The former terminology is

probably more appropriate, because the resistivity<sup>2</sup> increases linearly with  $T$  over a wide range of at least  $300\text{ K} < T < 550\text{ K}$  (See Fig. 1). The Hall number,  $n_H = 9 \times 10^{19}\text{cm}^{-3} = 0.05$  holes/cell, for the reported high  $ZT$  sample, although small for a metal may be too large to allow analysis of the transport in terms of usual semiconductor formulae. The Hall concentration calculated according to Eq.(5) is plotted in Fig.4 as a function of the Fermi level shift from its position in the stoichiometric compound. Note that  $n_H$  is not simply related to the actual number of holes; the experimental Hall number of 0.05 holes/cell corresponds to the doping level of 0.1 holes/cell, roughly twice  $n_H$ . Finally, the calculated plasma frequency at the same position of the Fermi level is  $\omega_p = 1 \sim 1.2\text{ eV}$  (depending on polarization), which corresponds to optical effective carrier concentration  $(n/m)_{\text{eff}} \approx 0.5(m_0/m)$  holes/cell with  $m_0$  being the bare electron mass. Analysis of the Fermi surface (see Fig. 5) shows that close to the top of the valence band in the range relevant to high  $ZT$  samples the main sheet of the Fermi surface is more toroidal rather than ellipsoidal. Thus even at this low carrier density, the Fermi surface has a complicated shape with electron-like and hole-like contributions to the Hall coefficient. This explains why the Hall concentration is so much different from the doping level, and also suggests that the Fermi velocity and conductivity may depend on the Fermi level position in a strong and unusual way. This is the case and it is partially responsible for the high thermopower.

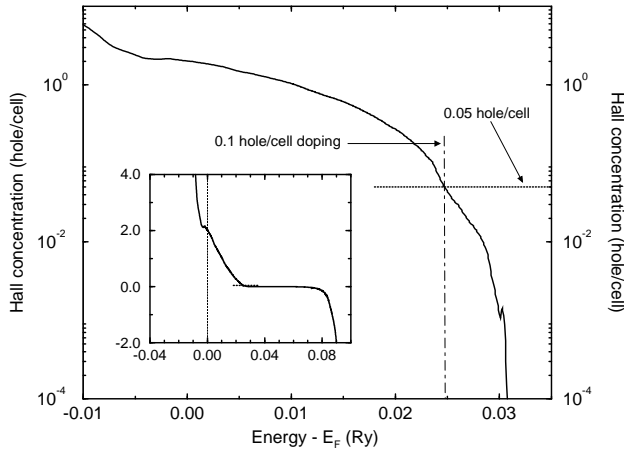


FIG. 4. Calculated Hall concentration as a function of the Fermi level position relative to the stoichiometric solid (solid line) in a linear-log plot. The inset shows the same quantity over wider range including both sides of the gap. The dotted horizontal line represents the experimental value and the dot-dashed vertical line denotes the required Fermi level shift to match the calculated Hall concentration to measured value.

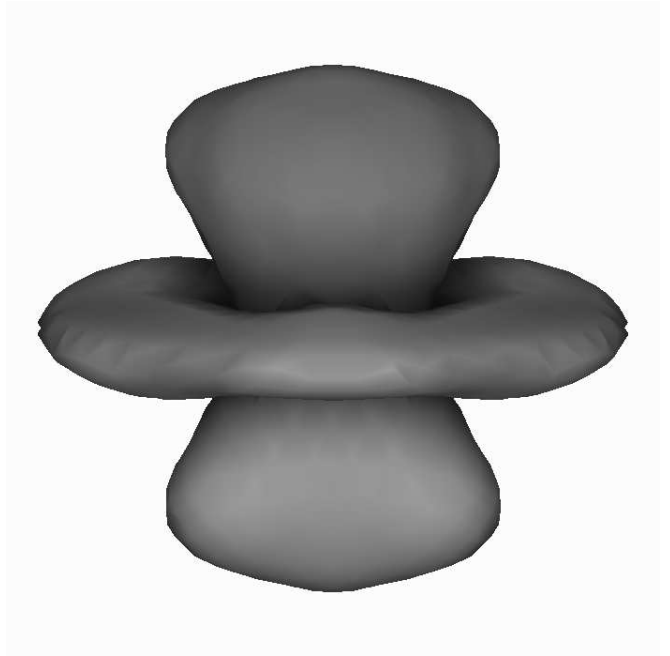


FIG. 5. Main Fermi surface of  $\beta\text{-Zn}_4\text{Sb}_3$  at the experimental band filling.

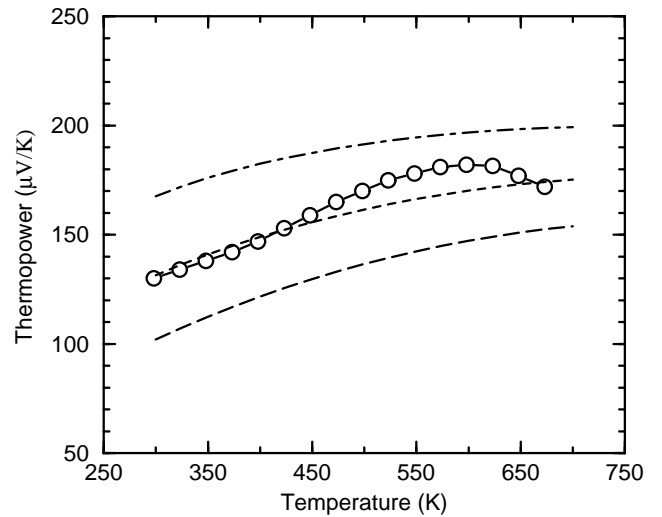


FIG. 6. Calculated (short dashes) and experimental (solid line with open circle) thermopower for  $\beta\text{-Zn}_4\text{Sb}_3$  with 0.05 hole/cell Hall concentration (0.10 hole/cell doping).  $S(T)$  for Hall concentrations 0.12 and 0.02 hole/cell (0.15 and 0.04 hole/cell doping level) are given by the curves above (dot-dashed) and below (long dashed) of those for the actual doping level for comparison.

Indeed, using Eq. (7), we find rather high Seebeck coefficient (Fig. 6). Naturally,  $S$  depends strongly on the

position of the Fermi level. Comparison with the experiment shows that very good agreement is achieved for the the hole count of 0.1 hole/cell. This is exactly the hole count that we deduced from the measured Hall number of 0.05 holes/cell, demonstrating the consistency of our approach.

As mentioned, the experimental resistivity up to approximately 550 K shows typical metallic behavior with high-temperature resistivity coefficient  $d\rho/dT \approx 3.1 \mu\Omega\text{-cm/K}$  and residual resistivity  $\rho_0 \approx 1.8 \text{ m}\Omega\text{-cm}$ . From these data and the calculated plasma frequency one can estimate the transport electron-phonon coupling constant  $\lambda_{\text{tr}}$  and the scattering rate  $\gamma$  due to static defects to obtain  $\lambda_{\text{tr}} \approx 1$ , and  $\gamma \approx 0.2 \text{ eV}$ . Both numbers are relatively large, but may represent overestimates since they are not based on single crystal data. In any case, the experimental data indicate that at high temperature  $\kappa$  is mainly  $\kappa_{\text{el}}$  in the best reported sample. This implies that variations in doping level that increase  $S$  will also increase  $ZT$ . Our calculations show not unexpectedly that raising the Fermi energy corresponding to lower carrier concentration, leads to higher values of  $S$ , particularly at intermediate temperatures ranging from room temperature to the maximum. This corresponds to higher Zn concentrations on the mixed site.

In summary, we have studied the band structures and transport properties of  $\beta\text{-Zn}_4\text{Sb}_3$  using first principles electronic structure calculations. According to our *ab initio* calculations, the Fermi surface has complicated topology and this makes the estimation of doping level non-trivial. Combining our calculations with the measured Hall number for the actual material, we arrive at a relatively large, essentially metallic, value for carrier concentration, 0.1 hole/cell. Using this, we calculated Seebeck coefficient and found it to be in excellent agreement with the experiment both in absolute value and temperature dependence. Based upon these results, we characterize this material as metal with complex, energy-dependent Fermi surface, which provides large thermopower for relatively high carrier concentration. This may be useful in identifying other candidate thermoelectric materials. The  $\beta\text{-Zn}_4\text{Sb}_3$  system is not yet optimized for thermoelectric application and further increase in  $ZT$  is expected if the doping level can be reduced. One important issue revolves around the question of why it is so difficult to make samples with varying Zn concentrations on the mixed site, since higher Zn concentration would lead to higher  $ZT$ . We speculate that the reason has to do with competition from other phases during the high temperature synthesis. It would be very interesting to attempt

growth by more non-equilibrium processes such as pulsed laser deposition.

The authors are grateful for helpful discussions with T. Caillat and J.P. Fleurial. Computations were performed using DoD HPCMO facilities at NAVO and ASC. This work is supported by DARPA. Work at NRL is supported by ONR.

- 
- <sup>1</sup> G. Mahan, B. Sales and J. Sharp, *Physics Today* **50** #3, 42 (1997).
  - <sup>2</sup> T. Caillat, J.P. Fleurial and A. Borshchevsky, *Proceedings ICT'96*, edited by T. Caillat, A. Borshchevsky and J.P. Fleurial (IEEE Press, Piscataway, 1996), p. 151.
  - <sup>3</sup> B.C. Sales, D. Mandrus and R.K. Williams, *Science* **272**, 1325 (1996).
  - <sup>4</sup> J.P. Fleurial, A. Borshchevsky, T. Caillat and G.P. Meisner, *Proceedings ICT'96*, edited by T. Caillat, A. Borshchevsky and J.P. Fleurial (IEEE Press, Piscataway, 1996), p. 91.
  - <sup>5</sup> D.J. Singh and I.I. Mazin, *Phys. Rev. B* **56**, R1650 (1994).
  - <sup>6</sup> L. Nordstrom and D.J. Singh, *Phys. Rev. B* **53**, 1103 (1996).
  - <sup>7</sup> D.J. Singh and W.E. Pickett, *Phys. Rev. B* **50**, 11235 (1994).
  - <sup>8</sup> J.L. Feldman and D.J. Singh, *Phys. Rev. B* **53**, 6273 (1996); **54**, 712 (1996).
  - <sup>9</sup> O.K. Anderson, *Phys. Rev. B* **12**, 3060 (1975).
  - <sup>10</sup> D.J. Singh, *Planewaves, Pseudopotential and the LAPW Method* (Kluwer, Boston, 1994).
  - <sup>11</sup> D.J. Singh, *Phys. Rev. B* **43**, 6388 (1991).
  - <sup>12</sup> L. Hedin and B.I. Lundqvist, *J. Phys. C* **4**, 2064 (1971).
  - <sup>13</sup> P. Villars and L.D. Calvert, *Pearson's Handbook of Crystallographic Data for Intermetallic Phases*, 2nd ed. (ASM International, Materials Park, OH, 1991), p. 5206.
  - <sup>14</sup> G.A. Slack, in *Solid State Physics*, edited by F. Seitz and D. Turnbull, Vol. 34 (Academic Press, New York, 1979), p. 1.
  - <sup>15</sup> D.G. Cahill, S.K. Watson and R.O. Pohl, *Phys. Rev. B* **46**, 6131 (1992).
  - <sup>16</sup> J.M. Ziman, *Principles of the Theory of Solids* (Cambridge University Press, Cambridge, 1972).
  - <sup>17</sup> C.M. Hurd, *The Hall effect in Metallic and Alloys* (Plenum, New York, 1972).
  - <sup>18</sup> W.W. Schulz, P.B. Allen and N. Trivedi, *Phys. Rev. B* **45**, 10886 (1992).
  - <sup>19</sup> A.E. Karakosov, I.I. Mazin and Y.A. Uspenski, *Sov. Phys. Doklady* **277**, 848 (1984).